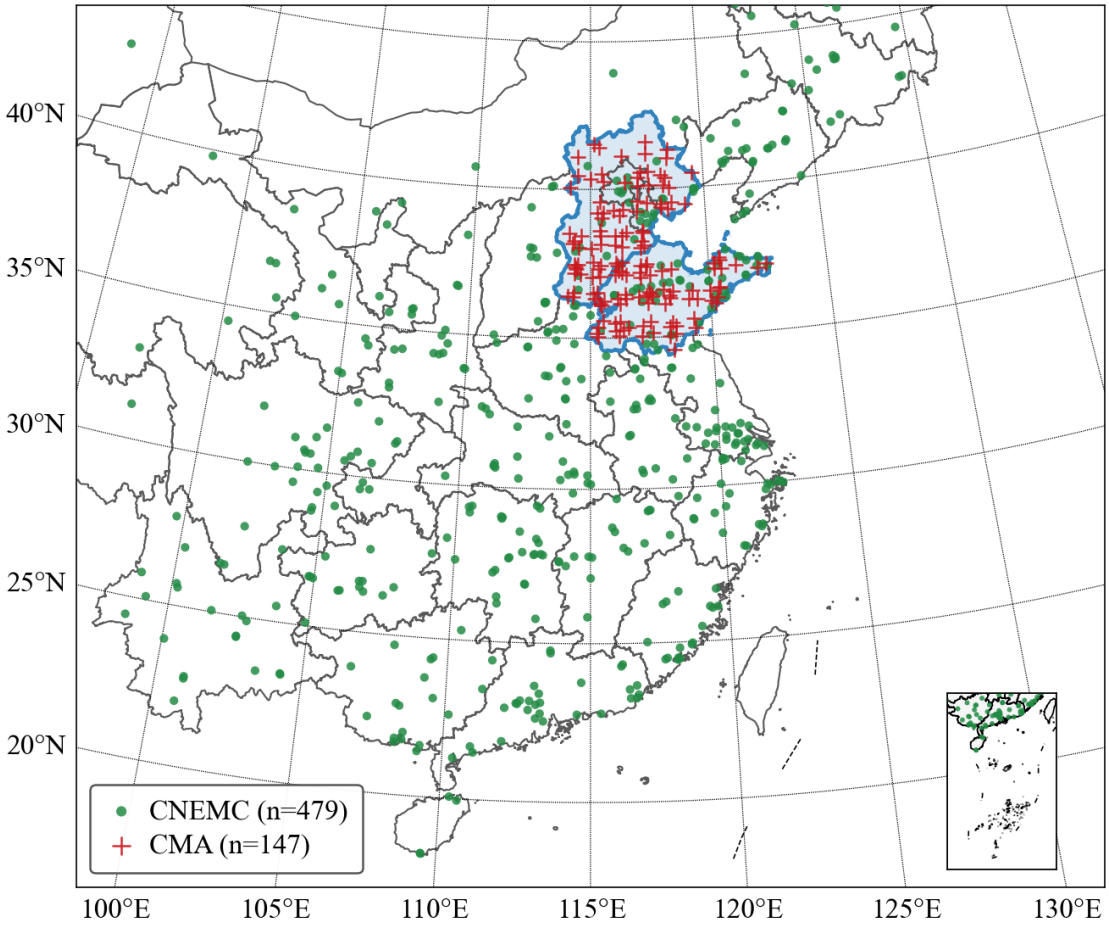

Figure S1 Model domain and the locations of two types of observation stations used in this study. Green circles denote CNEMC stations (n=479), while red crosses denote CMA stations (n=147).

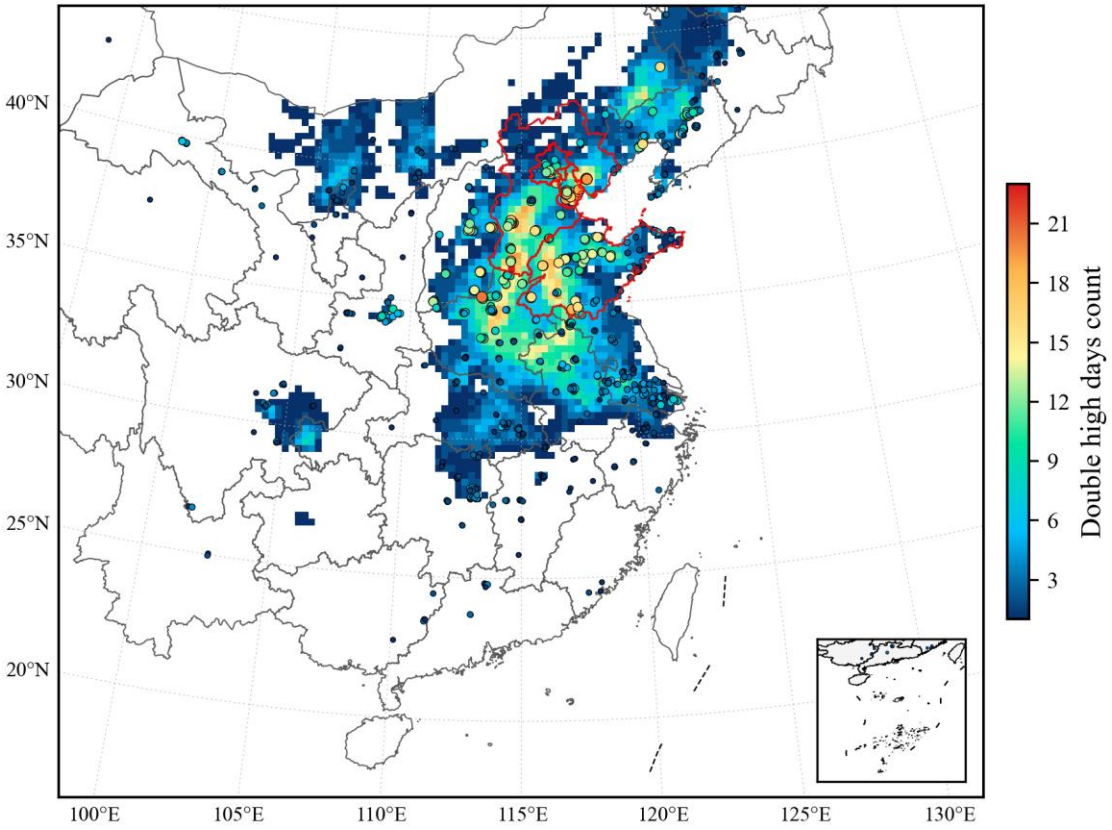

Figure S2 Spatial distribution of co-occurring $PM_{2.5}$ and O_3 pollution (DHP) days during 1–30 July 2020. A DHP day is defined as a day when the daily mean $PM_{2.5}$ exceeds 35 μg m^{-3} and the maximum daily 8-hour average (MDA8) O_3 exceeds 100 μg m^{-3} simultaneously. The color shading represents the number of DHP days at each WRF-Chem grid. Overlaid filled circles denote observed DHP days at surface observational stations, with the same color scale applied. The red outlines delineate the Beijing–Tianjin–Hebei-Shandong, where the most frequent co-pollution episodes are concentrated.

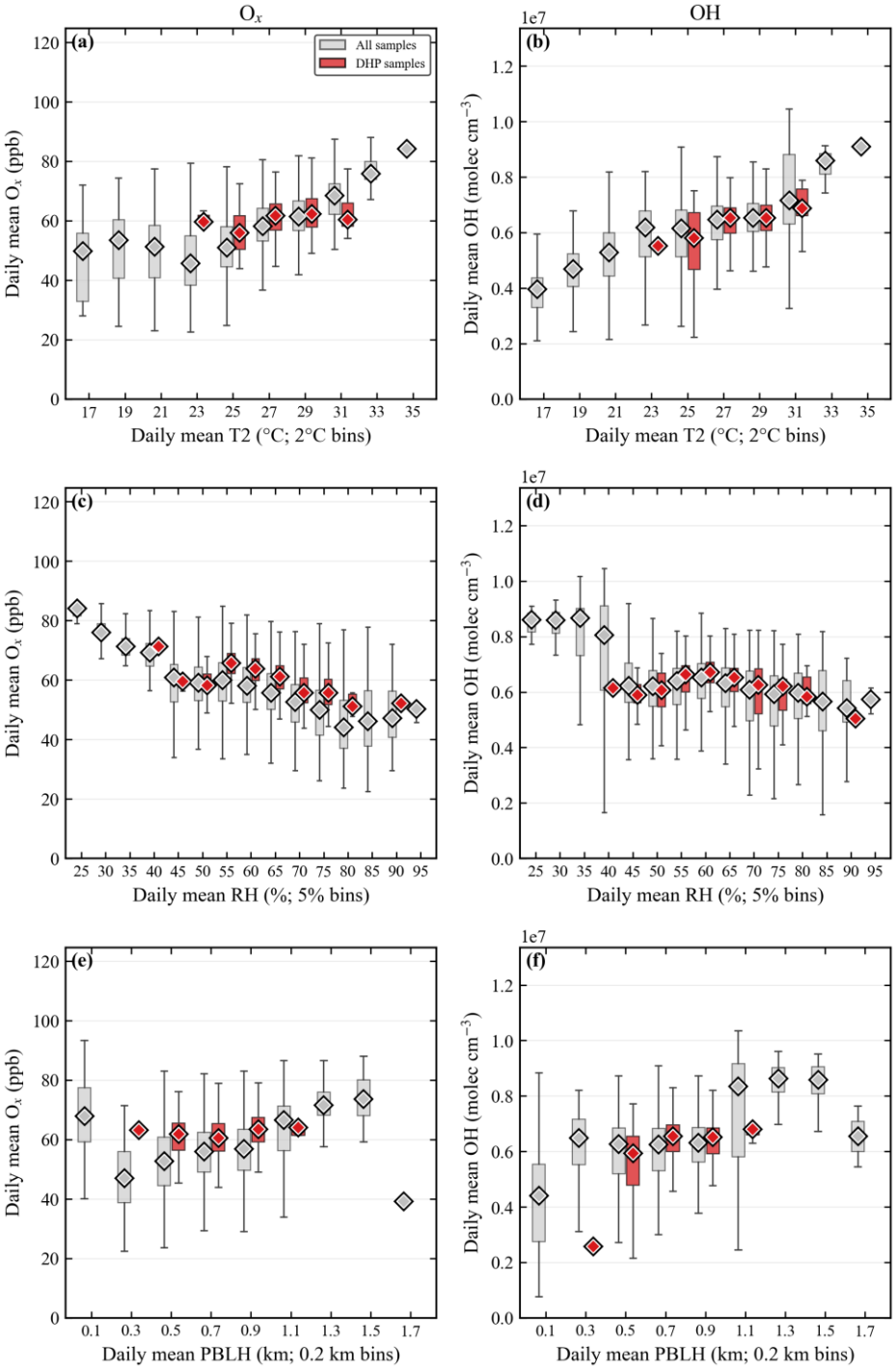

Figure S3 Boxplots of daily mean (a) (c) (e) Ox (O_3 + NO_2, ppb) and (b) (d) (f) OH (ppb) in each T2, RH2 and PBLH bin of all samples and DHP samples from the EXP_W_BASE experiment. T2 is binned to 2°C intervals, RH2 to 5% intervals and PBLH to 0.2km intervals. In each boxplot, the horizontal line inside the box represents the median, the box spans the interquartile range (25th–75th percentile), and the whiskers extend to the most extreme data points within 1.5 times the interquartile range from the box edges.

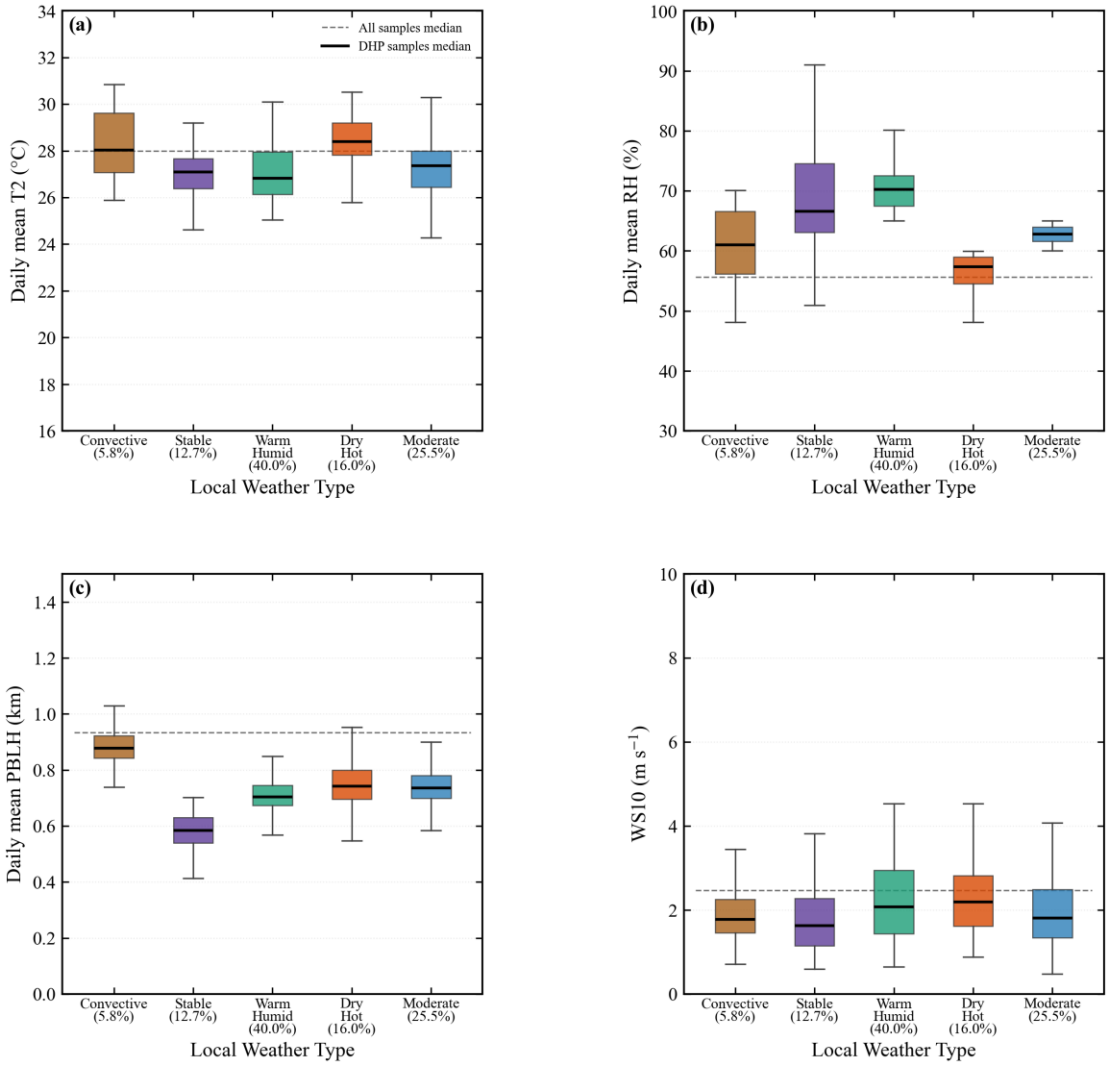

Figure S4 Boxplots of daily mean (a) 2-m air temperature (T2, °C), (b) relative humidity (RH, %), (c) planetary boundary layer height (PBLH, km), and (d) 10-m wind speed (WS10, m s^{-1}) for different meteorological condition types. The numbers in parentheses beneath each type indicate the proportion in the DHP samples and the gray dashed lines denote the median values for all samples.

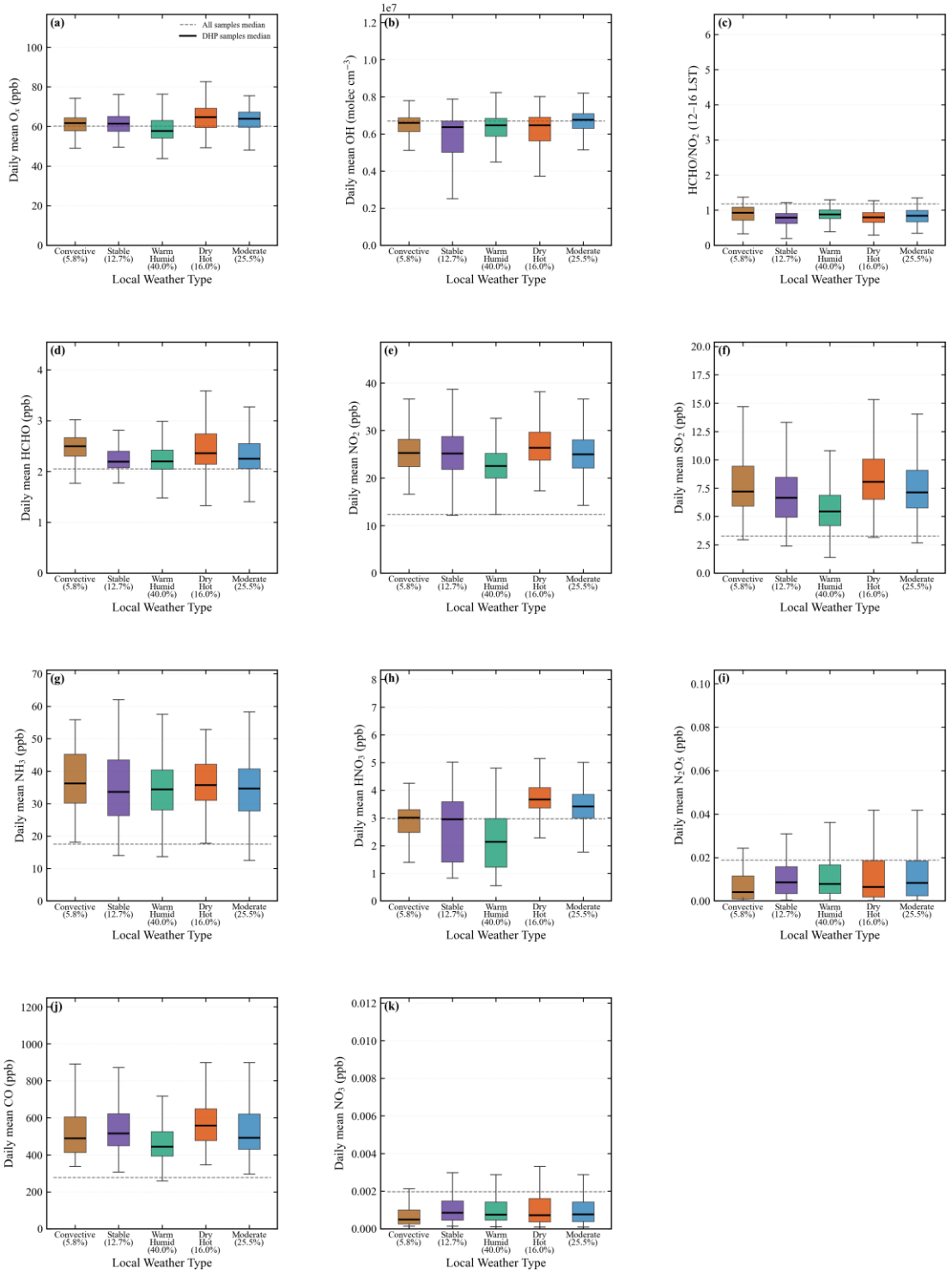

Figure S5 Boxplots of daily mean surface (a) total oxidants (Ox; ppb), (b) hydroxyl radicals (OH; molecule cm^{-3}), (c)$HCHO/NO_2$ ratio (unitless), (d) HCHO (ppb), (e) NO_2 (ppb), (f) SO_2 (ppb), (g) NH_3 (ppb), (h) HNO_3 (ppb), (i) N_2O_5 (ppb), (j) CO (ppb), and (k) nitrate radicals (NO_3; ppb) for different meteorological condition types. The numbers in parentheses beneath each type indicate the proportion in the DHP samples and the gray dashed lines denote the median values for all samples.

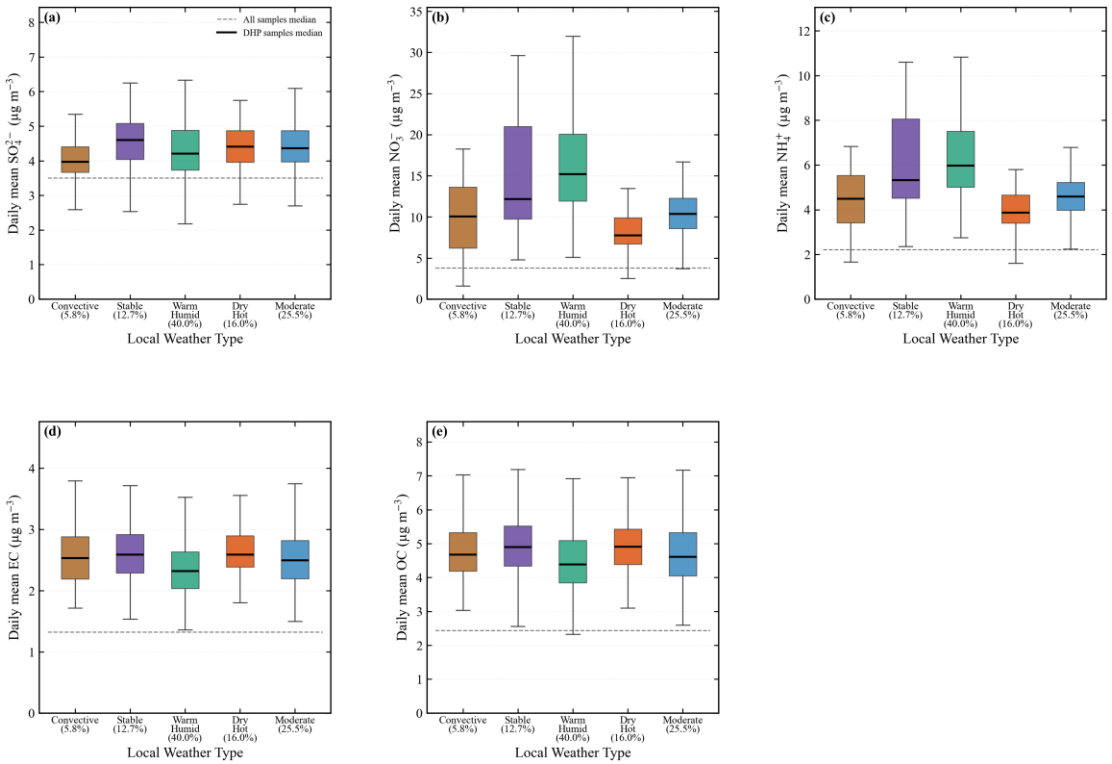

Figure S6 Boxplots of daily mean (a) SO_4^{2-} (μg m^{-3}), (b) NO_3^- (μg m^{-3}), (c) NH_4^+ (μg m^{-3}), (d) BC (μg m^{-3}), (e) OC (μg m^{-3}) for different meteorological condition types. The numbers in parentheses beneath each type indicate the proportion in the DHP samples and the gray dashed lines denote the median values for all samples.

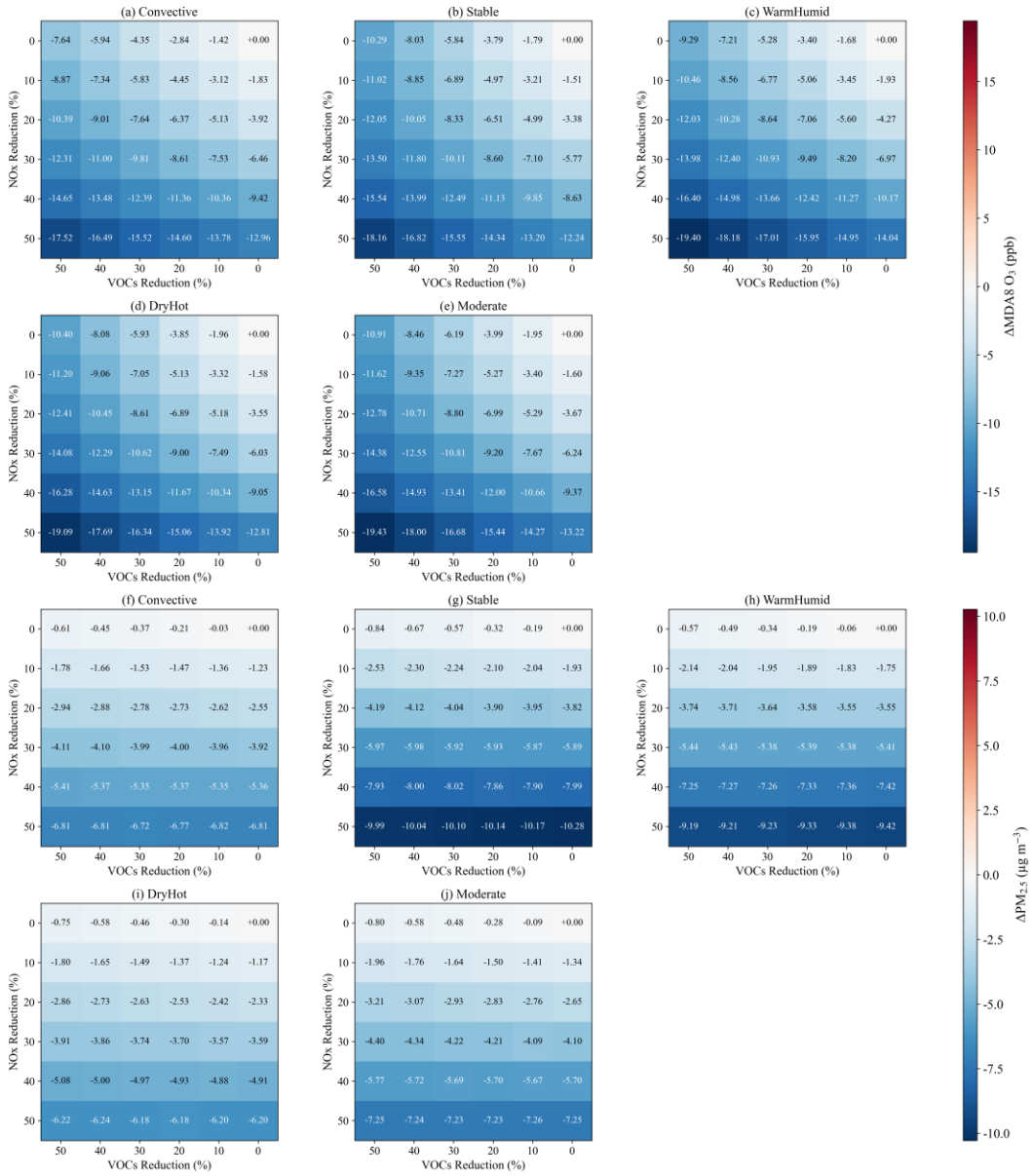

Figure S7 MDA8 O_3 and $PM_{2.5}$ response to NOx and VOC reductions for DHP samples classified into different meteorological condition types. The absolute differences in MDA8 O_3 between each reduction scenario and the baseline scenario (ΔMDA8 O_3, ppb) for (a) Convective, (b) Stable_Inv, (c) Neutral_WarmHumid, (d) Neutral_DryHot, and (e) Neutral_Cool conditions, and the absolute differences in $PM_{2.5}$ between each reduction scenario and the baseline ($\Delta PM_{2.5}$, μg m^{-3}) for (f) Convective, (g) Stable_Inv, (h) Neutral_WarmHumid, (i) Neutral_DryHot, and (j) Neutral_Cool conditions. Rows and columns denote NOx and VOC reduction levels (%).

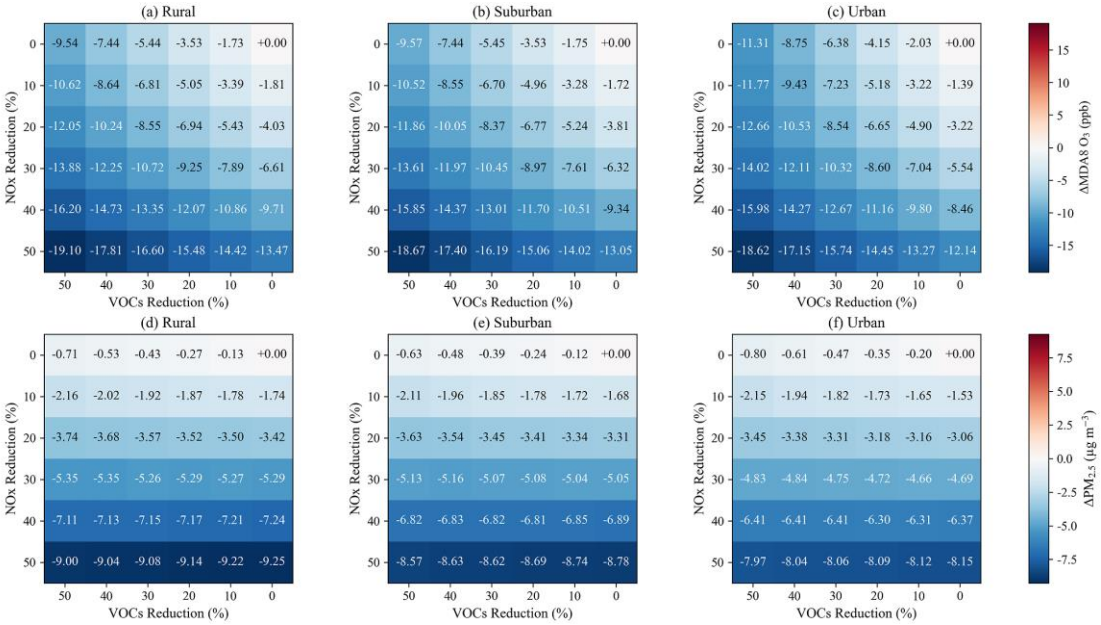

Figure S8 The absolute differences in MDA8 O_3 between each reduction scenario and the baseline scenario (ΔMDA8 O_3, ppb) for (a) Rural, (b) Suburban, and (c) Urban grid cells, and the absolute differences in $PM_{2.5}$ between each reduction scenario and the baseline ($\Delta PM_{2.5}$, μg m^{-3}) for (d) Rural, (e) Suburban, and (f) Urban grid cells for DHP samples. Rows and columns denote NOx and VOC reduction levels (%).

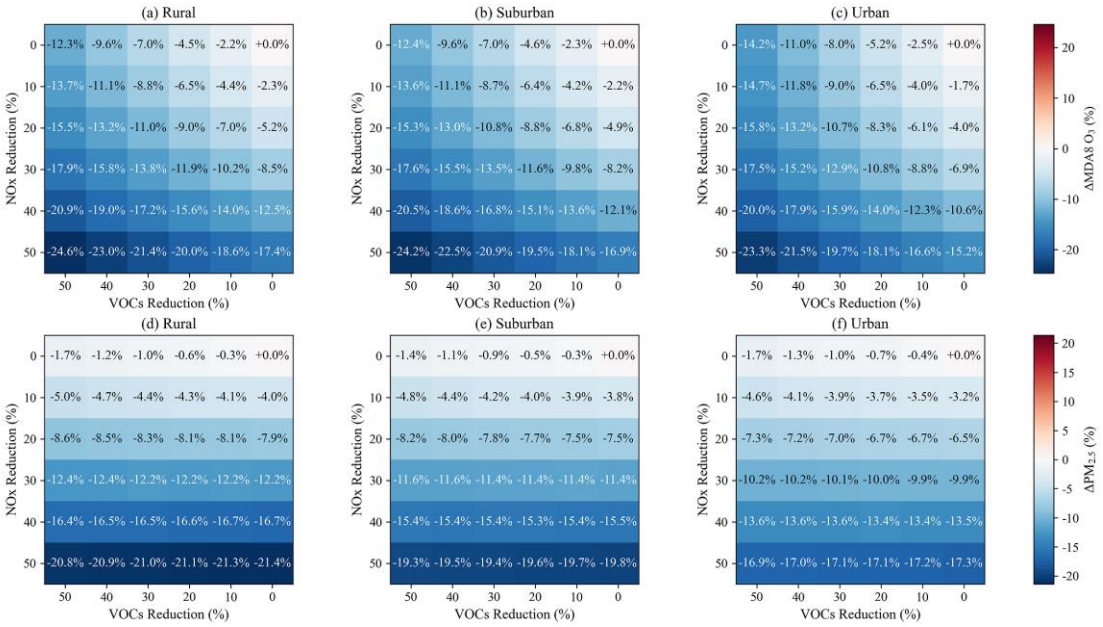

Figure S9 The percentage differences in MDA8 O_3 between each reduction scenario and the baseline scenario (ΔMDA8 O_3, %) for (a) rural, (b) suburban, and (c) urban grid cells, and the percentage differences in $PM_{2.5}$ between each reduction scenario and the baseline (Δ$PM_{2.5}$, %) for (d) rural, (e) suburban, and (f) urban grid cells for DHP samples. Rows and columns denote NOx and VOC reduction levels (%).

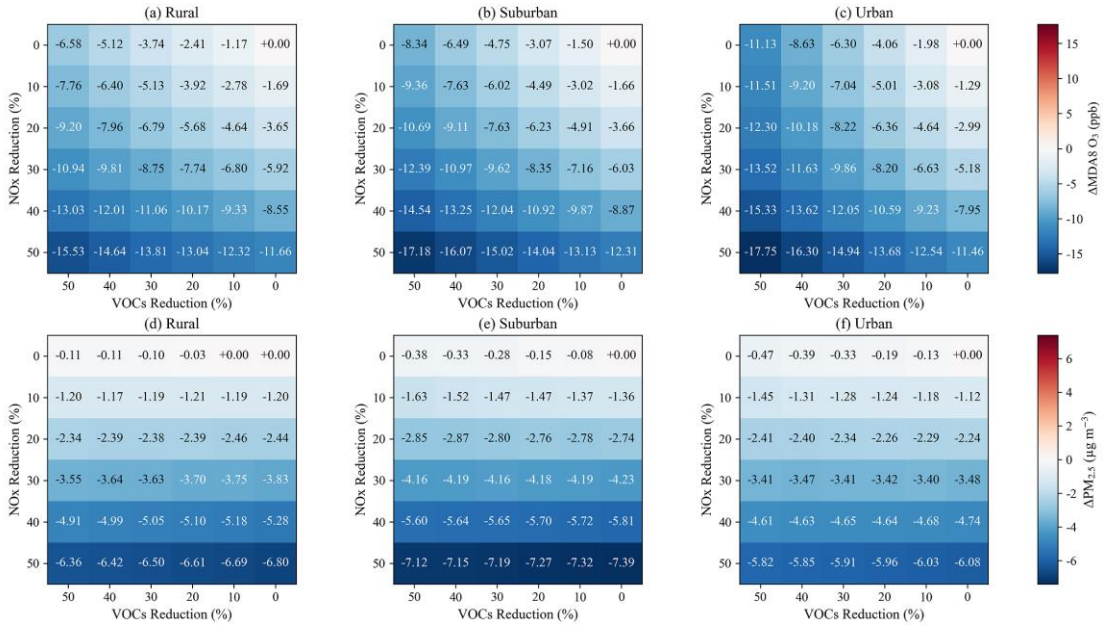

Figure S10 The absolute differences in MDA8 O_3 between each reduction scenario and the baseline scenario (ΔMDA8 O_3, ppb) for (a) Rural, (b) Suburban, and (c) Urban grid cells, and the absolute differences in $PM_{2.5}$ between each reduction scenario and the baseline($\Delta PM_{2.5}$, μg m^{-3}) for (d) Rural, (e) Suburban, and (f) Urban grid cells for all samples. Rows and columns denote NOx and VOC reduction levels (%).

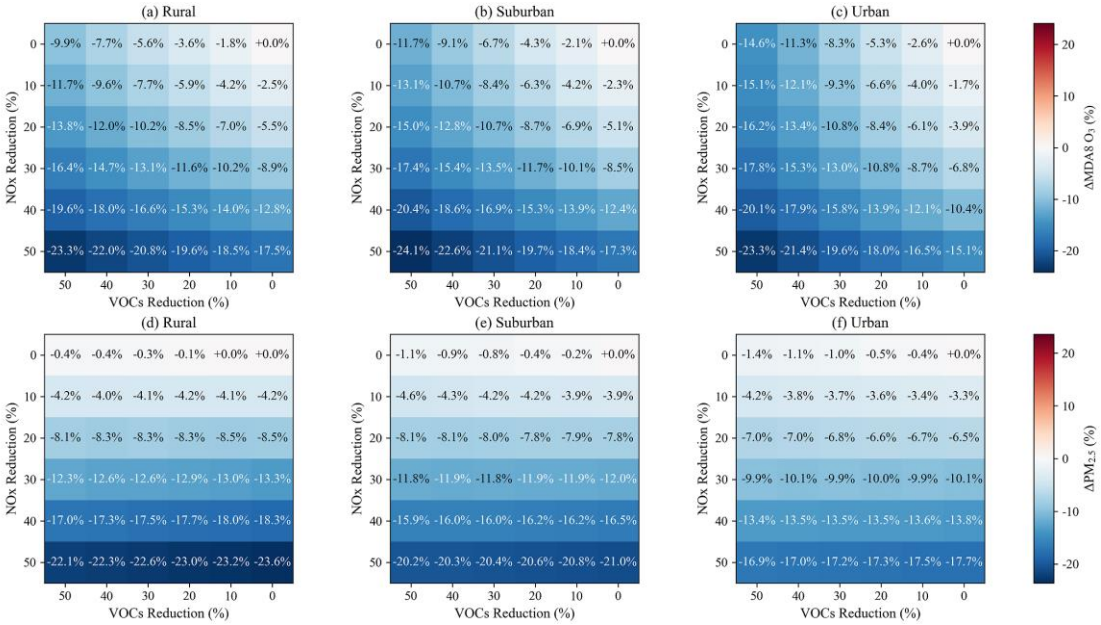

Figure S11 The percentage differences in MDA8 O_3 between each reduction scenario and the baseline scenario (ΔMDA8 O_3, %) for (a) Rural, (b) Suburban, and (c) Urban grid cells, and the percentage differences in $PM_{2.5}$ between each reduction scenario and the baseline ($\Delta PM_{2.5}$, %) for (d) Rural, (e) Suburban, and (f) Urban grid cells for all samples. Rows and columns denote NOx and VOC reduction levels (%).

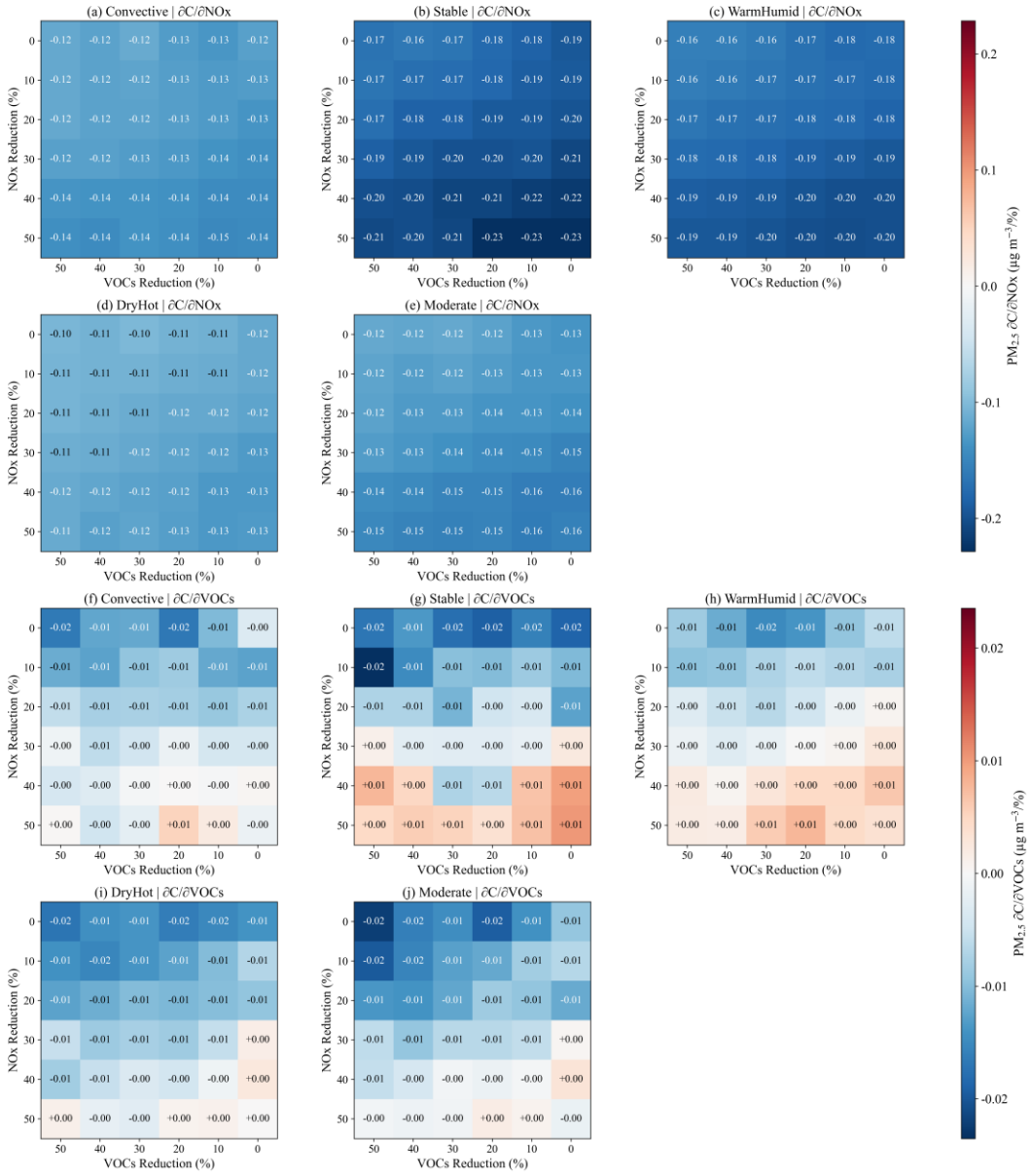

Figure S12 $PM_{2.5}$ response gradient to NOx and VOC emission reductions for DHP samples classified into different meteorological condition types. $\partial(PM_{2.5})/\partial NOx$ (μg m^{-3}/%) for (a) Convective, (b) Stable, (c) WarmHumid, (d) DryHot, and (e) Moderate, and $\partial(PM_{2.5})/\partial VOCs$ (μg m^{-3}/%) for (a) Convective, (b) Stable, (c) WarmHumid, (d) DryHot, and (e) Moderate. The gradients are computed by differentiating the absolute response matrices with respect to the reduction level at 10 percentage point intervals (0, 10, 20, 30, 40, 50%). Rows and columns denote NOx and VOC reduction levels (%).

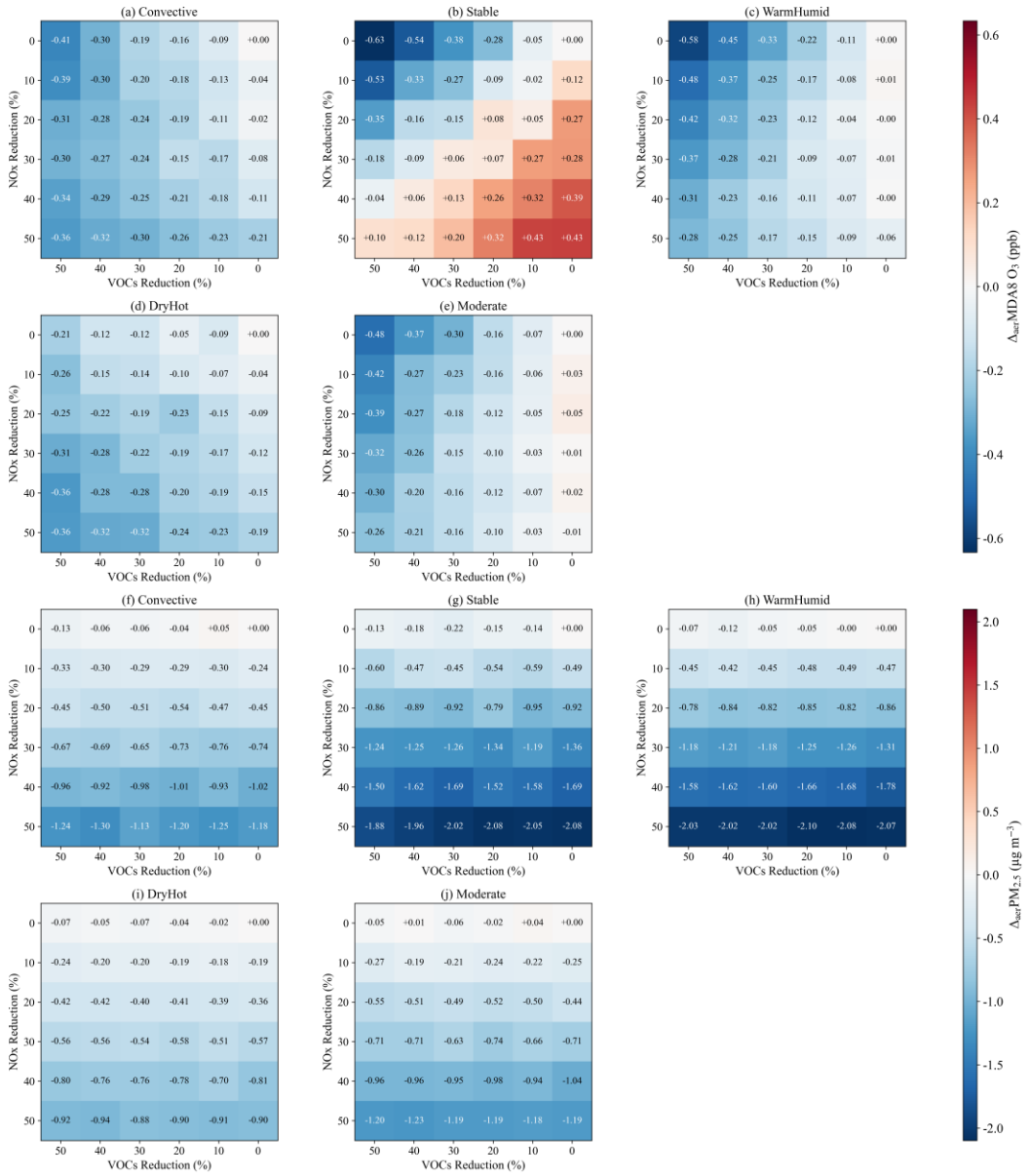

Figure S13 Aerosol-induced absolute change of MDA8 O_3 (Δ_{aer}MDA8 O_3, ppb) and $PM_{2.5}$ ($\Delta_{aer}PM_{2.5}$, μg m^{-3}) responses to NOx and VOC emission reductions for (a) (f) Convective, (b) (g) Stable, (c) (h)WarmHumid, (d) (i) DryHot, and (e) (j) Moderate. Rows and columns denote NOx and VOC reduction levels (%), respectively.